

Electrodeposition of Silver Amalgam Particles on Screen-Printed Silver Electrodes in Voltammetric Detection of 4-nitrophenol and Artificial Nucleosides dTPT3 and d5SICS

Pavlina Havranova^a, Lukas Fojt^a, Lukas Kejik^{a,b,c}, Tomas Sikola^{b,c}, Miroslav Fojta^a, Ales Danhel^{a}*

^a Institute of Biophysics of the Czech Academy of Sciences, Kralovopolska 135, CZ-61265 Brno, Czech Republic

^b Central European Institute of Technology, Brno University of Technology, Purkynova 123, CZ-612 00 Brno, Czech Republic

^c Institute of Physical Engineering, Brno University of Technology, Technicka 2, CZ-616 69 Brno, Czech Republic

* e-mail: danhel@ibp.cz

Abstract

Electrodeposition of silver amalgam particles (AgAPs) on various substrates offers perspective tool in development of novel electrochemical detection system applicable even in direct bioelectrochemistry of nucleic acids or proteins. Herein, a double pulse chronoamperometric deposition of AgAPs on in-house fabricated screen-printed silver electrodes (SPAgE) has been optimized using voltammetric signal of model electrochemically reducible organic nitro-compound, 4-nitrophenol, and scanning electron microscopy with energy dispersive X-ray spectrometer. This compact sensor including graphite counter and Ag|AgCl pseudo-reference electrode was design for highly effective analysis of electrochemically reducible compounds in 96-well plate with about 150- μ l sample volume per well. The SPAgE-AgAP offers detection of 4-NP down to 5 μ mol.l⁻¹ using cyclic voltammetry in acetate buffer pH 5.0. Advantageously, differential pulse voltammetry at SPAgE-AgAP allows highly sensitive detection system of unnatural nucleosides dTPT3 and d5SICS, which successfully expanded genetic alphabet of recently studied semi-synthetic organism, with limits of detection 0.1 pg. μ l⁻¹ in 0.05 mol.l⁻¹ hydrochloric acid. Moreover, these artificial nucleosides are detectable in the mixture with natural nucleosides up to weight ratio 1 : 15 000. SPAgE-AgAP may be potentially utilized in simple, fast and sensitive electrochemical detection of organic nitro compounds and free or in DNA harbored dTPT3 and/or d5SICS, what may contribute in successful research and development of semi-synthetic organism perspective in chemical and synthetic biology.

Keywords: Silver; 4-nitrophenol; Silver amalgam; Voltammetry; dTPT3; d5SICS

Highlights:

- Screen printed silver electrodes (SPAgE) represent suitable substrate for electrodeposition of silver amalgam particles (AgAP)
- Amalgam composition and morphology of the electrode surface was observed by scanning electron microscopy with energy dispersive X-ray spectroscopy
- SPAgE-AgAP represents novel compact electrode system for electrochemically reducible organic compounds in about 150- μ l sample volume
- SPAgE-AgAP allowed detection of dTPT3 and d5SICS by means of differential pulse voltammetry down to 0.1 $\text{pg}\cdot\mu\text{l}^{-1}$
- dTPT3 and d5SICS are detectable in mixture with natural nucleotides (dNs) down to 1:15 000 weight ratio (dTPT3 or d5SICS : dNs)

1. Introduction

Electrodeposition of silver amalgam particles (AgAPs) on various substrates was found to be perspective approach for development of novel (spectro-)electroanalytical systems applicable in detection of electrochemically reducible compounds, nucleic acids or proteins [1-4]. Moreover, AgAPs were confirmed as a suitable material for introduction of plasmonic functionalities into photochemical and spectro-electrochemical systems [5]. Until recently, electrochemical studies, following AgAPs deposition on selected substrates from a deposition solution of Ag^+ and Hg^{2+} , required additional reference and counter electrodes. This increases demands on total volume of the deposition and sample solution down to minimum of 1 ml. Implementation of a three-electrode system to one portable sensor by taking advantage of screen-printed technology could overcome these issues, simplify preparation procedure, and significantly decrease consumption of the deposition and sample solutions. Therefore, for the first time in this work, compact in-house fabricated screen-printed electrodes (smaller than the most of the commercial ones) were applied for AgAPs deposition and further detection of selected analytes inside of the one of 96-well plate containing about 150 μl of the solutions.

Screen-printing technology allows a mass production of highly reproducible, disposable, single-use screen-printed electrodes at a reduced cost in general. An additional advantage of screen-printing consists in possible implementation of a variety of configurations with different electrode geometries and sizes. The composition of the various inks used for printing of the electrodes is the most critical factor that determines the selectivity and sensitivity of detection. Great versatility of the printing inks is based on their bulk- or surface-modification by the

addition of different compounds (metals, enzymes, polymers, complexing agents *etc.*) [6]. Surface modification of screen-printing electrodes by electrodeposited AgAPs has never been studied before according to our best of knowledge. Since AgAPs have proven to be suitable for the surface modification of transparent indium-tin oxide (ITO) [1], vapor deposited golden thin film (vAuE) [2] or pyrolytic graphite (PG) [3], herein in-house fabricated screen-printed silver electrode with silver composite working electrode (SPAgE) has been selected as novel substrate for AgAPs deposition. This metal silver based substrate should also minimize risk of mercury contamination, thank to high mercury affinity to the silver substrate, and thus increased mechanical stability and about two orders of magnitude lowered mercury vapor pressure [7]. For all the above mention substrates, the AgAPs modification has significantly facilitated electro-reduction of organic nitro compounds [1] and additionally allowed detection of labeled [2] or even unlabeled nucleic acids [3] or proteins [4]. Analogical effects are expected in case of AgAPs electrodeposition on SPAgE, but detail study and optimization are needed. This compact and mechanically stable sensor could advantageously be also used for detection of artificial nucleobases dTPT3 and d5SICS, which in pairs with dNaM broaden genetic alphabet within the research and development of semi-synthetic organisms (SSO) [8-10]. There are high demands on sensitive analytical techniques for determination of these artificial bases. Fast, cost effective, and sufficiently accurate and sensitive detection system minimizing sample volume consumption could significantly contribute in the progress of the SSO research. Spacek has already developed an electrochemical method for both, free or even harbored dTPT3 and d5SICS within SSOs' plasmid DNA using differential pulse voltammetry (DPV) at hanging mercury drop electrode (HMDE). Thanks to strong adsorption affinity of the artificial bases to mercury surfaces and their capability of catalytic hydrogen evolution reaction on HMDE, highly sensitive voltammetric method has been developed and applied for their detection. An applicability of silver amalgam electrodes has also been proposed as an alternative in the work [11].

Therefore, the aim of this work was to optimize double pulse chronoamperometric (DPCA) electrodeposition of AgAPs on the in-house fabricated SPAgEs designed for batch voltammetric detection of electrochemically reducible compounds inside of the one of 96-well plate containing 150- μ l of sample per well. Since the SPAgEs have been used as the substrates for the first time in this work, the AgAPs electrodeposition procedure and resulting detection system has been optimized using well electrochemically studied model organic nitro-compound, 4-nitrophenol (4-NP) and scanning electron microscopy with energy dispersive X-ray spectrometer (SEM-EDS). After that, practical applicability of the herein presented SPAgE-

AgAP has been demonstrated by voltammetric detection of the artificial nucleosides dTPT3 and d5SICS, free or next to the natural nucleosides in the mixtures.

2. Experimental

2.1 Chemicals and reagents

Solution of 0.01 mol.l^{-1} AgNO_3 (p.a. 99.8% Safina) in 0.1 mol.l^{-1} KNO_3 (p.a. >98%, Fluka) was used. Solution of 0.01 mol.l^{-1} $\text{Hg}(\text{NO}_3)_2$ in 0.1 mol.l^{-1} KNO_3 was prepared according to procedure described in Ref. [2]. The 0.001 mol.l^{-1} stock solution of 4-NP (p.a., >99%, Sigma-Aldrich) was prepared in deionized water. Natural nucleosides (Sigma), dTPT3 and d5SICS (Berry and Associates) were diluted in DMSO (99.9% Sigma Aldrich) to 0.010 mol.l^{-1} . All solutions were prepared using deionized water (Millipore, Milli-Q water system). Other chemicals were of analytical grade.

2.2 Preparation of screen-printed silver electrodes

Screen-printed silver electrodes (SPAgEs) involved silver working electrode (diameter = 2.0 mm), graphite counter electrode and $\text{Ag}|\text{AgCl}$ pseudoreference electrode. The SPAgEs were printed in-house on polycarbonate foil (0.375 mm thick, Sabic), which has been cleaned by isopropyl alcohol and demineralized water before the printing process, by the Horizon 8 (DEK) screen printing machine using the following pastes: $\text{Ag}(60\%)|\text{AgCl}(40\%)$ (C2130809D5, Gwent); 65% silver (C2081126P2, Gwent), graphite (BQ242, Dupont) and insulating one (D2071120P1, Gwent). The graphite ink was used as conductor for the silver electrode.

2.3 Electrodeposition of AgAPs

Electrodeposition of the silver amalgams (AgAPs) was carried out under the air by DPCA from net 0.01 mol.l^{-1} $\text{Ag}^+/\text{Hg}^{2+}$ in 0.1 mol.l^{-1} KNO_3 . The SPAgE was used without prior pretreatment as the compact sensor including three electrode system.

2.4 Voltammetric measurement

All electrochemical measurements were carried out by Autolab PGStat128N operated by Nova Software Ver. 1.10 or GPES software Ver. 4.9 (all Metrohm-Autolab). Cyclic voltammetry (CV) measurements of 4-nitrophenol were performed with initial potential (E_i) -0.1 V , switching potential (E_{sw}) -1.2 V , scan rate 0.1 V.s^{-1} , and in background electrolyte 0.2 mol.l^{-1}

acetate buffer (AcP) pH 5.0. Detection of dTPT3 and d5SICS was performed in 50 mol.l⁻¹ HCl by differential pulse voltammetry (DPV) with E_i -0.5 V, final potential (E_f) -1.5 V, step potential 0.5 mV, modulation amplitude 25 mV, modulation time 0.01 s, interval time 0.1 s (corresponding scan rate 5 mV.s⁻¹). The solution was purged with argon (5.0 purity, AirProducts) before each measurement. All experiments were performed at room temperature.

2.5 SEM-EDS analyses

The morphology of the samples was investigated by SEM (FEI Verios 460L) equipped with an EDS system (EDAX SDD Octane Super). The acceleration voltage of 6.0 kV and beam current of 0.80 nA were applied. Ag L α , Hg M α and Au M α spectral lines were used for the EDS quantification using peak-to-background PeBaZAF method with a correction for rough surfaces/particles.

3. Results and Discussion

3.1 Substrate

Electrochemical behavior and stability of the substrate provides basic information about exploitable potential window which may significantly influence final application of the sensor with electrodeposited AgAPs. This has been found essential mainly in e.g. DNA or protein electroanalysis^[3], which requires electrochemically stable substrate providing a broad negative potential window. Anodic and cathodic parts of potential windows of already studied substrates (ITO, gold or pyrolytic graphite) are limited by anodic dissolution (oxidation) of electrodeposited AgAPs and by hydrogen evolution proceeding either on the substrate or AgAPs, respectively. This depends on relative surface coverage (a ratio between AgAPs' and substrate surface areas) of the AgAPs on the substrate, since silver amalgam offers the hydrogen overpotential as comparably negative as metal mercury and thus more negative than ITO, gold or pyrolytic graphite. Here it should be reminded, that ITO is reduced before hydrogen evolution reaction and thus applicable potential window is significantly limited (from about +0.1 to -1.0 V)^[1]. It has been experimentally found, that electrochemical reactions including hydrogen evolution prevail on AgAPs, when the relative surface coverage exceeds 40%. Exploitable potential windows (herein defined by the limiting current densities (j) ± 5 mA.cm⁻² vs. Ag|AgCl|3M KCl) of bare substrates in 0.1 mol.l⁻¹ KNO₃ solutions as well as AgAPs' decorated ones in 0.2 mol.l⁻¹ AcP pH 5.0 are summarized in Table 1.

Table 1. Potential windows (E_{win}) of selected substrates and cathodic peak potentials (E_p^c) corresponding to Ag^+ and Hg^{2+} reductions on the substrates in $0.1 \text{ mol.l}^{-1} \text{ KNO}_3$, and E_{win} of the substrates with electrodeposited AgAPs (using selected conditions optimized in corresponding Ref.). E_{win} were determined using limiting current densities $\pm 5 \text{ mA cm}^{-2}$ and all the potentials are related to $Ag|AgCl|3 \text{ mol.l}^{-1} \text{ KCl}$.

Electrolyte		0.1 mol.l ⁻¹ KNO ₃		AcP pH 5.0	
Substrate	E_{win}/V	$E_p^c(Ag^+)/V$	$E_p^c(Hg^{2+})/V$	E_{win}/V	Ref.
ITO(-AgAP)	+1.75...-1.63	+0.205	-0.120	+0.05...-1.16*	[1]
vAuE(-AgAP)	+0.53...-1.12	+0.240	+0.305	+0.25...-1.43*	[2]
bPGE(-AgAP)	+0.45...-1.80	+0.215	+0.340	+0.35...-1.70*	[3]
SPAgE	+0.51...-1.45	+0.260	+0.340	+0.32...-1.43	This work
SPAgE-AgAP	---	---	---	+0.45...-1.63	This work

*at the substrate decorated by AgAPs

Since SPAgE offer potential window just about 100 mV narrower than PG at negative potentials and this up to now nonstudied metal silver based working electrode All the substrates with or without electrodeposited AgAPs exceed -1.5 V of applicable potential windows are promising for bioelectroanalysis.

3.2 Electrochemical behavior of Ag^+ and Hg^{2+} at SPAgE

Affinity of the metal silver and mercury obviously influenced reducibility of the metals on the substrates (see reduction peak potentials in Tab. 1). Therefore their cyclic voltammograms were registered using SPAgE. Moreover, the knowledge of the reduction potentials of Ag^+ and Hg^{2+} then help us to select appropriate intervals for selection of nucleation and growth potentials, which have also been optimized (Fig. 1).

Reducibility of the metals on selected substrates follow the order: vAuE>PGE>>SPAgE>>ITO. then following order The bare SPAgE provides potential window within +0.42 and -1.45 V in $0.1 \text{ mol.l}^{-1} \text{ KNO}_3$. electrochemical behaviour of the Ag^+ , Hg^{2+} ions and their mixture (Ag^+/Hg^{2+} , 30.6 w%_{Ag}) were individually studied using cyclic voltammetry within potential ranges of +0.5 V to -0.5 V or +0.5 to -1.5 V at SPAgE. CVs were measured in the solutions containing $0.01 \text{ mol.l}^{-1} \text{ AgNO}_3$, $Hg(NO_3)_2$ or their mixture containing 30.6% Ag (w/w) in $0.1 \text{ mol.l}^{-1} \text{ KNO}_3$. Silver ions produced cathodic peak at -200 mV at SPAgE and mercury produced cathodic peak at -150 mV (Fig. 1).

Voltammograms of $\text{Ag}^+/\text{Hg}^{2+}$ mixture were analogous to voltammograms of single metals and allowed us to select suitable potentials for electrodeposition of AgAP on SPAGE. According to this CV, intervals of nucleation ($E_1 = \{-1.0; -1.5\}$ V) and grow potentials ($E_2 = \{-0.1; -0.5\}$ V) of DPCE could be selected in consideration of the negative end of the potential window limited by H^+ reduction, and of the Ag^+ and Hg^{2+} reduction at bare SPAGE, respectively.

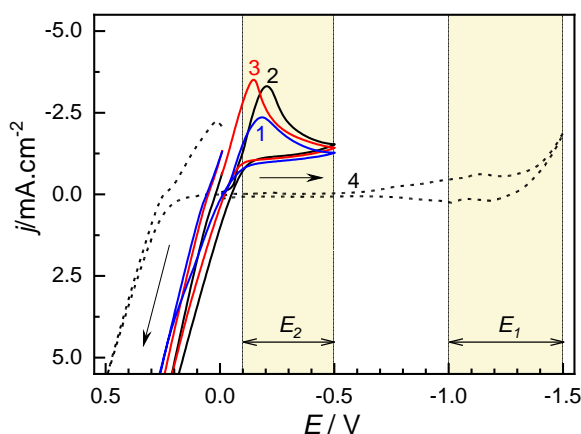


Fig. 1 Cyclic voltammograms of: $0.01 \text{ mol.l}^{-1} \text{ AgNO}_3$ (1), $0.01 \text{ mol.l}^{-1} \text{ Hg(NO}_3)_2$ (2), $0.01 \text{ mol.l}^{-1} \text{ AgNO}_3 + \text{Hg(NO}_3)_2$ 30.6 w% $_{\text{Ag}}$ (3) registered at bare SPAGE in $0.1 \text{ mol.l}^{-1} \text{ KNO}_3$ (4). E_i 0.0 V, first E_{sw} -0.5 V or -0.5 V for (4), second E_{sw} 0.5 V, E_f 0.0 V, scan rate 0.1 V.s^{-1} . The yellow areas depict intervals of DPCE's nucleation (E_1) and growth (E_2) potentials optimized in Chap 3.3.

3.2 Influence of solution constitution

In analogy with results obtained for preparation of silver amalgam particles on ITO^[1] and gold^[2] and pyrolytic graphite electrodes^[3], DPCE was selected as suitable method for electrodeposition of AgAP on SPAGE. During the optimization of the electrodepositions, various Ag/Hg ratio in solution and different parameters of chronoamperometry (pulse (E_1) and grow (E_2) potentials and times (t_2)) were used.

Influence of various Ag/Hg ratio in the solution was studied as the first parameter of AgAP deposition. In agreement with result of CV measured in the solutions containing $0.01 \text{ mol.l}^{-1} \text{ AgNO}_3$ and $\text{Hg(NO}_3)_2$ and with our previous work^[2] nucleation potential (E_1) -1.1 V applied for nucleation time (t_1) ($t_1 = 50$ ms was kept constant during all the experiments), followed by growth potential (E_2) -0.2 V lasting growth time (t_2) 60 s, were selected at the beginning. Content of the Ag^+ in the solution varied between 0 – 100 w% $_{\text{Ag}}$, whereas the mercury ions constituted the rest and net content of both metals was kept constant at 0.01 mol.l^{-1} . Amalgams morphology and constitution were observed by SEM-EDS. SEM micrographs of the resulting

electrodes (Fig. 2) reveal the significant difference in the morphology of the prepared AgAP particles based on the solution composition. Small particles with higher uniformity were observed for the deposition solutions with silver concentration in the range of 40 – 75 w%_{Ag}. The EDS analyses showed the constitution of the particles prepared from solution containing less than 40 w%_{Ag} were different from constitution of the solutions. On the contrary quantity of the Ag in particles prepared from solution containing more than 40 w%_{Ag} responded with solution constitutions Fig. 2). The CVs of 4-NP on these electrodes (Fig. 3) offered strong and well-developed peaks for AgAP prepared from solutions containing more than 30 w%_{Ag}. Therefore, only solutions containing 30.6, 39.7, 50.0 and 61.7 w%_{Ag} were selected for further optimization of DPCA parameters in following Chapter 3.3.

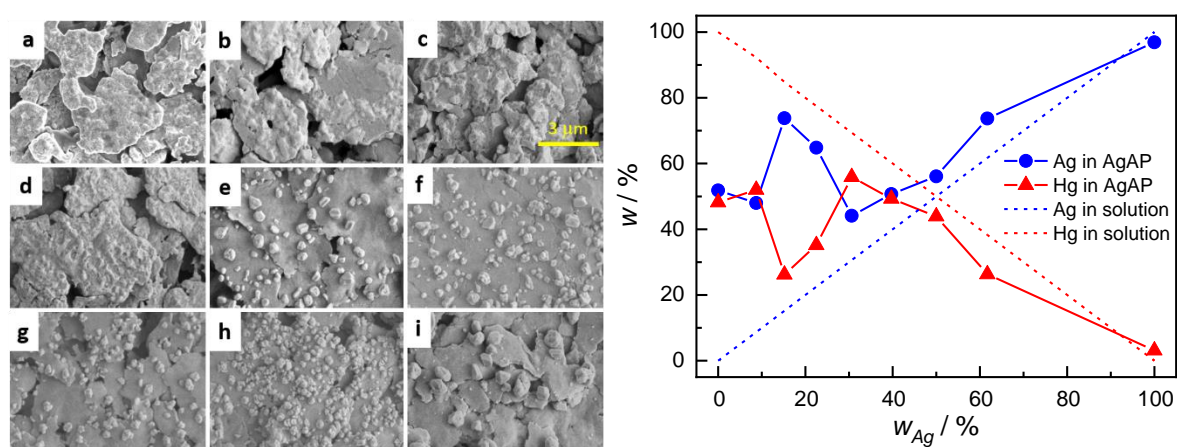


Fig. 2. (Left) SEM micrographs of AgAPs electrodeposited onto SPAGE from deposition solution containing (w_{Ag} in %): 0.0 (a), 8.7 (b), 15.2 (c), 22.5 (d), 30.6 (e), 39.7 (f), 50.0 (g), 61.7 (h) and 100.0 w%_{Ag} (i), using DPCA ($E_1 = -1.1$ V, $t_1 = 50$ ms, $E_2 = -0.2$ V and $t_2 = 60$ s), scale bar 3 μm. (Right) Influence of electrodeposited amalgam's composition (w) on solution constitution (w_{Ag}) resulting from EDS analysis. Straight lines indicate the content of the metals in the deposition solution.

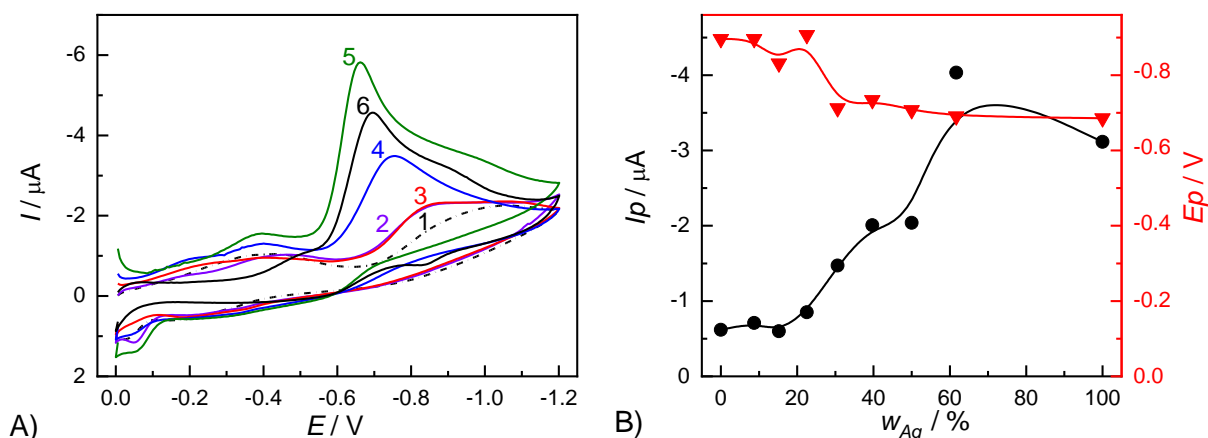


Fig. 3. (A) Cyclic voltammograms of $100 \mu\text{mol.l}^{-1}$ 4-NP in AcB (scan rate 0.1 V s^{-1}) registered by SPAgE-AgAP prepared by DPCA using $E_1 = -1.1 \text{ V}$, $t_1 = 50 \text{ ms}$, $E_2 = -0.2 \text{ V}$ and $t_2 = 60 \text{ s}$, from the solution containing: 0.0 (1), 8.7 (2), 22.5 (3), 39.7 (4), 61.7 (5) and 100.0 w% Ag (6) in $0.1 \text{ mol.l}^{-1} \text{ KNO}_3$. (B) Extracted 4-NP peak currents (I_p) and peak position (E_p) evaluated from the CVs (A) registered on SPAgE-AgAP.

3.3 Optimization of electrodeposition parameters

Knowledge of the electrochemical reducibility of Ag^+ and Hg^{2+} at the substrate then provides information about selection of proper potential ranges of nucleation and growth potentials utilized for DPCA electrodeposition of AgAPs on SPAgE. These parameters were optimized and discussed in Chap 3.3.

The DPCA parameter E_1 was optimized using the deposition solution containing 30.6, 39.7, 50.0 and 61.7 w%_{Ag}. Composition of the electrodeposited AgAP remained constant within the range of E_1 -1.0 to -1.5 V and responded with composition of used Ag/Hg solutions (Fig. 6). SEM images of the electrodeposited AgAPs obtained during optimization of E_1 are shown on Fig. 5. Effects of E_1 on electrochemical behavior of prepared AgAP were studied by CV of 4-NP in AcB (Fig. 6A). The smallest particles with higher uniformity were observed for solution constitution 61.7 w%_{Ag} and E_1 -1.1 V . With using these parameters, the highest and most pronounced CV peak of 4-NP were observed, therefore solution containing 61.7 w%_{Ag} and E_1 -1.1 V were selected for optimization of E_2 and t_2 .

Dependences of intensity of 4-NP peaks on E_2 and t_2 are shown on Fig. 6B. Height of 4-NP peaks increased within the range of t_2 30 s to 180 s and remained constant or degraded for t_2 longer than 180 s for all used E_2 . The highest peak 4-NP was observed for DPCA parameters: $E_1 = -1.1 \text{ V}$, $t_1 = 50 \text{ ms}$, $E_2 = -0.5 \text{ V}$ and $t_2 = 180 \text{ s}$. These parameters were therefore selected for the subsequent measurements of 4-NP concentration dependences and repeatability in

following Chapter 3.4 and for electrochemical detection of unnatural nucleosides dTPT3 and d5SICS discussed in Chapter 3.5. SEM micrographs of SPAgE and SPAgE-AgAP and comparison of 4-NP peaks measured on SPAgE and SPAgE-AgAP (prepared with selected parameters) is shown on Fig. 5.

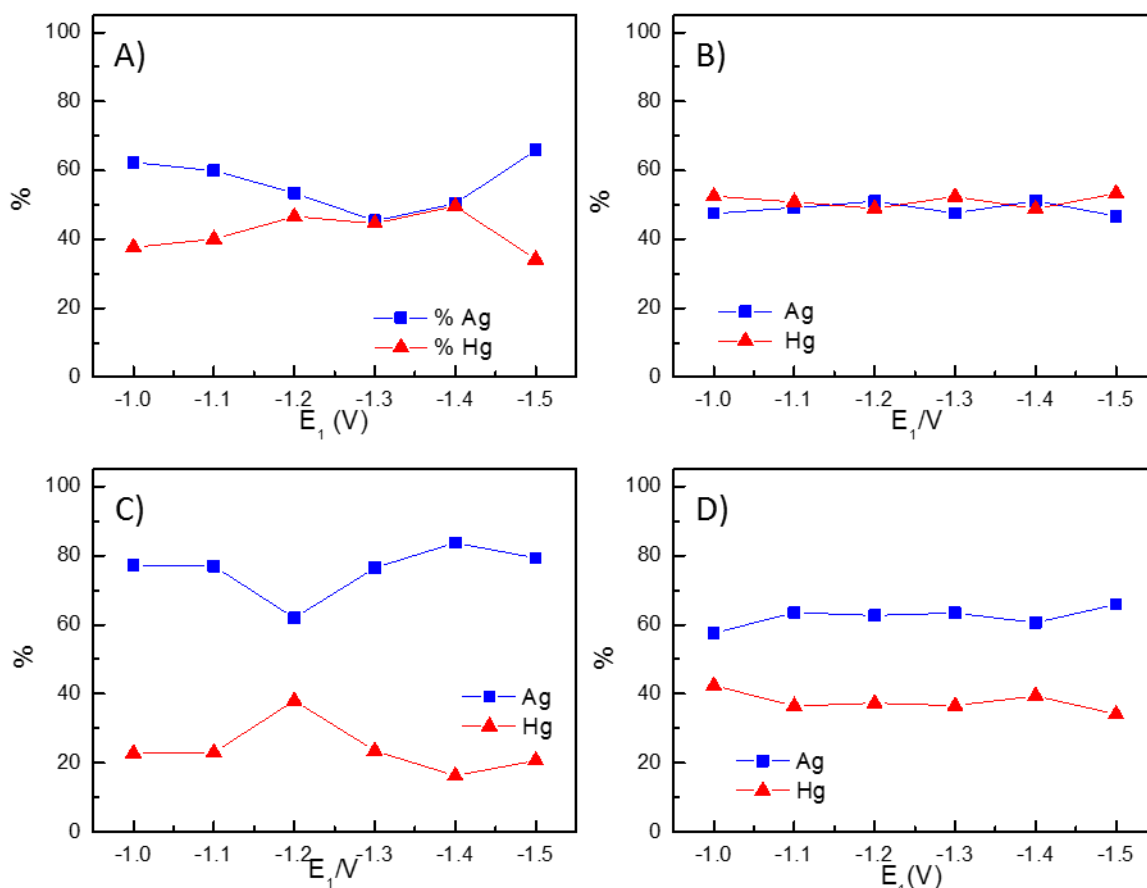


Fig. 4. Influence of nucleation potential (E_1) on constitution of AgAP prepared by DPCA using variable E_1 , $t_1=50$ ms, $E_2=-0.2$ V and $t_2=60$ s, from the solution containing: 30.6 (A), 39.7 (B), 50.0 (C) and 61.7 w%_{Ag} (D) resulting from EDS analysis.

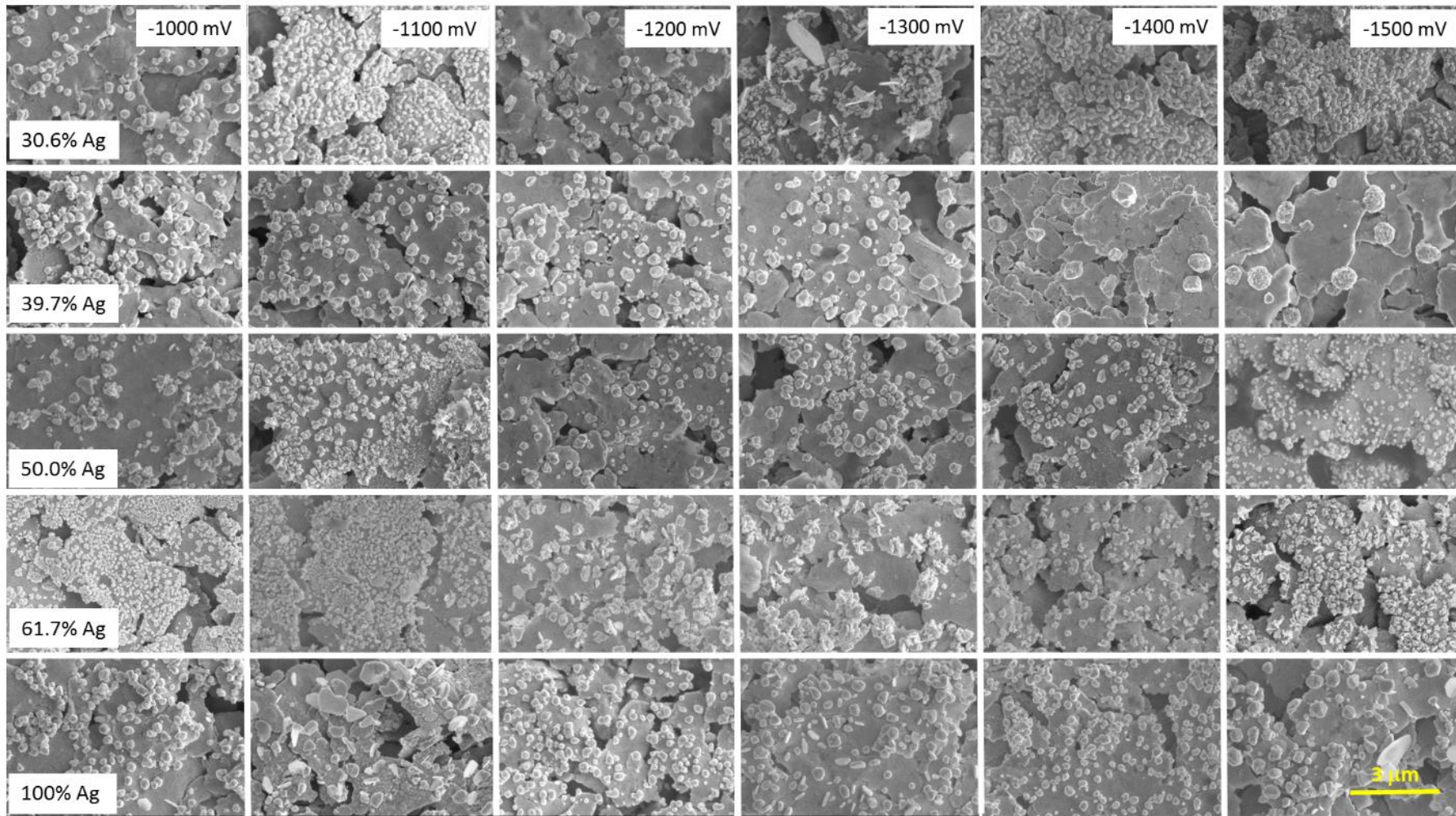


Fig. 5. SEM micrographs of AgAPs electrodeposited onto SPAGe from solution containing various w_{Ag} using DPCA with various E_1 ($t_1 = 50$ ms, $E_2 = -0.2$ V and $t_2 = 60$ s), scale bar 3 μm .

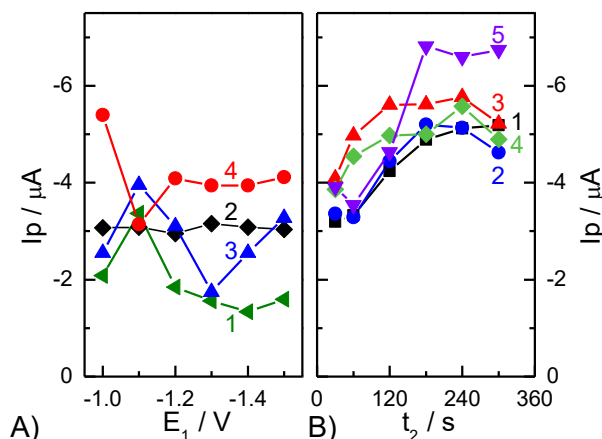


Fig. 6. (A) Influence of nucleation potential (E_1) on 4-NP peaks current (I_p) registered at SPAgE-AgAP prepared by DPCA with variable E_1 and $t_1=50$ ms, $E_2=-0.2$ V and $t_2=60$ s, from the solution containing: 30.6 (1), 39.7 (2), 50.0 (3) 61.7 w%_{Ag} (4). (B) Influence of peak current on grow time (t_2) registered by SPAgE-AgAP prepared by DPCA from solution containing 61.7 w%_{Ag} using $E_1=-1.1$ V, $t_1=50$ ms, and variable E_2 (V): -0.1 (1), -0.2 (2), -0.3 (3), -0.4 (4) and -0.5 V (5).

3.4 Voltammetric detection of 4-nitrophenol

We investigated the repeatability of the AgAP electrodeposition and 4-NP detection. Deposition of AgAP followed by CV detection of 4-NP were repeated twelve times. Every repetition was done on the new SPAgE. The resulting relative standard deviation (RSD) of the 4-NP's CV signal was 9% (Fig. 7b).

Applicability of optimized AgAP-AgAP in electroanalysis, concentration dependences of the 4-NP were registered by CV (Fig. 7). Measurement of every concentration were three times repeated with RSD not exceeding 10% for all concentration of 4-NP. Parameters of the linear fit of the concentration line are: slope = $-0.0420 \pm 0.00117 \mu\text{A} \cdot \text{l} \cdot \mu\text{mol}^{-1}$, intercept = $-0.622 \pm 0.046 \mu\text{A}$, $R^2 = 0.9938$, resulting limits of detection (LoD, calculated as $\text{LoD} = 3 \times \text{Signal/Noise}$) is $1 \mu\text{mol} \cdot \text{l}^{-1}$ (Fig. 7a).

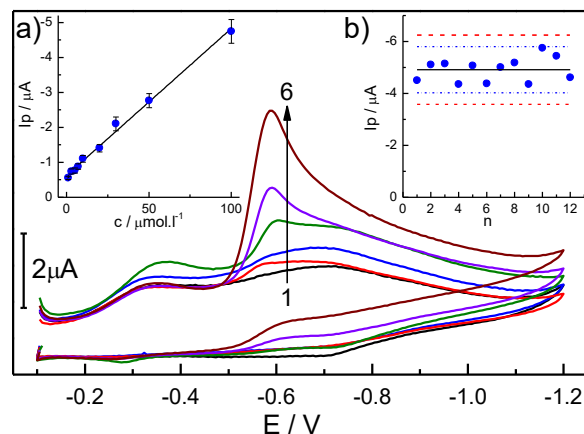


Fig. 7. Cyclic voltammograms of 4-NP in dependence on its concentration: 0 (1); 1 (2); 5 (3); 10 (4); 50 (5) and 100 $\mu\text{mol.l}^{-1}$ (6), measured at SPAgE-AgAP (DPCA: $E_1 = -1.1$ V, $t_1 = 50$ ms, $E_2 = -0.5$ V and $t_2 = 180$ s) in AcB pH 5.0. (Inset A) Extracted concentration dependences on 4-NP peaks heights (I_p) and (Inset B) Regulation diagram of twelve-time repeated CV detection of 4-NP ($100 \mu\text{mol.l}^{-1}$) by SPAgE-AgAP (eachery detection was performed by new SPAgE-AgAP) representing evaluated peak current (I_p) and average (solid black line) together with warning (dash dot blue lines, $\pm 2 \times \text{SD}$) and regulation limits (dash red line, $\pm 3 \times \text{SD}$).

3.5 Voltammetric detection of dTPT3 and d5SICS

A semi-synthetic organisms have been shown to replicate, transcribe and translate unnatural base pairs (UBPs) harbored within their plasmid DNA [9,10,12]. Expanded genetic code of semi-synthetic organisms enables production of proteins containing coded unnatural amino acid and could help deepen our understanding of life and its underlying mechanisms. Unnatural base pair formed aromatic nucleobase analogues dNaM -dTPT3 and dNaM -d5SICS (Fig. 8). Analytical method currently used for detection of UBPs are liquid chromatography, a streptavidin gel shift mobility assay and Sanger sequencing [8,13].

In our work we developed a novel method of electrochemical analyses of UBPs based on hydrogen catalysis by TPT3 and 5SICS on the surface of SPAgE-AgAP. AgAP were prepared by DPCA using $E_1 = -1.1$ V, $t_1 = 50$ ms, $E_2 = -0.5$ V and $t_2 = 180$ s. Constitution of Ag/Hg solution were optimized for dTPT3 detection. Content 15.2 w%_{Ag} were developed as the most appropriate Ag/Hg ratio in solution.

Electrochemical behavior of unnatural nucleosides dTPT3 and d5SICS were studied by DPV on the SPAgE-AgAP in 50 mmol.l^{-1} HCl. Both dTPT3 and d5SICS produced catalytic peaks at -1.2 V. A detailed view of the measured catalytic peaks as a function of dTPT3 and d5SICS concentration is shown on Fig. 9AB (electrolyte was subtracted from DPV graph of dTPT3

and d5SICS). Extracted concentration dependences of currents and positions of peaks dTPT3 and d5SICS are shown on Fig. 9CD. Parameters of the linear fit of the concentration lines in the range 0.1 – 1.0 $\text{pg}\cdot\mu\text{l}^{-1}$, together with the resulting limits of detection (LoD, calculated as $\text{LoD}=3\times\text{Signal}/\text{Noise}$), are summarized in Tab. I. These experiment proved that SPAgE-AgAP can be useful for DPV-based detection of dTPT3 and d5SICS down to 0.1 $\text{pg}\cdot\mu\text{l}^{-1}$.

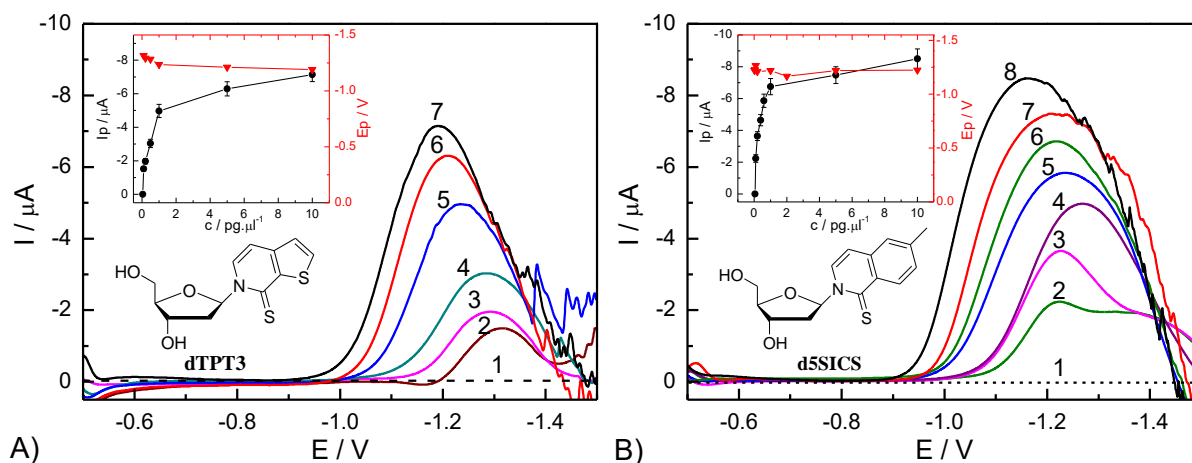


Fig. 6. Baseline corrected DP voltammograms of dTPT3 (A, chemical structure inside) in dependence on concentration ($\text{pg}\cdot\mu\text{l}^{-1}$): 0.05 (1), 0.1 (2), 0.2 (3), 0.5 (4), 1.0 (5), 5.0 (6) and 10.0 $\text{pg}\cdot\mu\text{l}^{-1}$ (7) and d5SICS (B, chemical structure inside): 0.05 (1), 0.1 (2), 0.2 (3), 0.4 (4), 0.6 (5), 1.0 (6), 5.0 (7) and 10.0 $\text{pg}\cdot\mu\text{l}^{-1}$ (8) with in the inset extracted concentration dependences of peak currents (I_p) and potentials (E_p), measured at SPAgE-AgAP (DPCA: $E_1=-1.1$ V, $t_1=50$ ms, $E_2=-0.5$ V and $t_2=180$ s, from 15.2 w%Ag in 0.1 $\text{mol}\cdot\text{l}^{-1}$ KNO_3) in 50 $\text{mmol}\cdot\text{l}^{-1}$ HCl as a base electrolyte. DP voltammograms of the lowest concentration 0.05 $\text{pg}\cdot\mu\text{l}^{-1}$ of dTPT3 and d5SICS were subtracted from all the DP voltammograms of dTPT3 and d5SICS, respectively.

Table 2. Parameters of the linear fit of concentration lines for detection of dTPT3 and d5SICS using DPV at SPAgE-AgAP, all measured in 0.05 $\text{mol}\cdot\text{l}^{-1}$ HCl.

Nucleoside	Slope ($\mu\text{A}\cdot\mu\text{l}\cdot\text{pg}^{-1}$)	intercept (μA)	R^2	Range ($\text{pg}\cdot\mu\text{l}^{-1}$)	LoD ($\text{pg}\cdot\mu\text{l}^{-1}$)
dTPT3	-7.203 ± 0.498	-0.322 ± 0.028	0.9719	0.1 – 1.0	0.1
d5SICS	-6.1633 ± 1.015	-1.653 ± 0.571	0.8565	0.1 – 1.0	0.1

Voltammetric detection of dTPT3 and d5SICS in surplus of natural nucleosides (dNs) were examined with using DPV analysis in 50 $\text{mmol}\cdot\text{l}^{-1}$ HCl of mixtures dTPT3/dNs and d5SICS/dNs in ratios 1:100, 1:1000, 1:5000, 1:10000 and 1:15000, concentration of all nucleosides was 2 $\text{ng}\cdot\mu\text{l}^{-1}$. Measurement of every mixture were tree times repeated with RSD

around 10% for all mixtures. A detailed view of the DPV of dTPT3 and d5SICS in mixtures with dNs and natural dNs are shown on Fig. 10AB (electrolyte was subtracted from DPV graph of all mixtures). Both TPT3 and 5SICS catalytic peaks were observed for mixtures with dTPT3 (d5SICS)/dNs ratio 1:100 – 1:10000. In DPV of mixtures with ratio 1:15000 catalytic peaks were not observed. Extracted currents and positions of peaks dTPT3 and d5SICS in mixtures with natural dNs are shown on Fig. 10CD. Parameters of the linear fit of lines of DPV peaks of dTPT3 and d5SICS in the mixtures are summarized in Tab. 3.

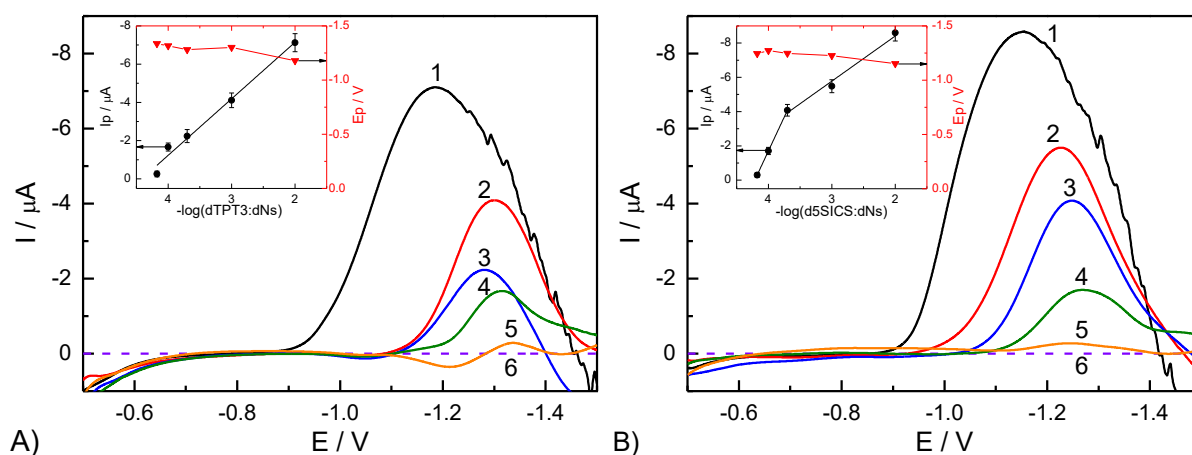


Fig. 7. DPV voltammograms of dTPT3/dNs (A) and d5SICS/dNs (B) mixture in dependence on dTPT3:dNs or 5SICS:dNs ratio: dNs (dash line), 1:100 (1), 1:1000 (2), 1:5000 (3), 1:10000 (4), 1:15000 (5) and the only dNs (6), with (Insets) linear dependences of peak currents (I_p) and potentials (E_p) on negative logarithm of the dTPT3:dNs or 5SICS:dNs ratios. More details see in Fig. 6. DP voltammograms of the dNs were subtracted from all the DP voltammograms of dTPT3 and d5SICS.

Table 3. Parameters of the linear fit of DPV peak currents and negative logarithm of dTPT3:dNs or d5SICS:dNs ratios.

Nucleoside	Slope (μA)	Intercept (μA)	R^2	dTPT3:dNs or d5SICS:dNs range
dTPT3	2.96 ± 0.21	-13.05 ± 0.73	0.9803	1:100 – 1:15 000
d5SICS	2.36 ± 0.33	-13.7 ± 1.0	0.9695	1:100 – 1:5 000
	7.923 ± 0.036	-33.39 ± 0.15	0.9999	1:5 000 – 1:15 000

Conclusion

This work confirmed the SPAGE as suitable platform for direct electrodeposition of silver amalgam particles from small volume of the solution decreasing its consumption. Simultaneous electro-reduction of silver and mercury ions could be applied for preparation of nanostructured

and sufficiently stable silver amalgam particles with controllable distribution and surface coverage. Its electroanalytical application was proved by detection of dTPT3 and d5SICS. dTPT3 and d5SICS were detected down to concentration $0.1 \text{ pg. } \mu\text{l}^{-1}$ both pure and in surplus of natural dNs. Its application in analyses of modified DNA will be the scope of further research.

Herein implemented SPAGE-AgAP and developed method of dTPT3 and d5SICS detection could contribute in further development of semi-synthetic organism. This approach significantly decreases consumption of deposition solution and decrease demands on minimal sample volume, what could increase AgAPs' application opportunities in bioelectroanalysis. Herein developed system provides perspective advantage in (bio)electroanalysis by simultaneous employment of multichannel potentiostat moreover what would significantly increase throughput of the analysis. This method may play a role in development of SSO and their further application in chemical and synthetic biology.

Acknowledgements

This work has been supported by a Grant Agency of the Czech Republic (project 17-23634Y) and by the SYMBIT project reg. no. CZ.02.1.01/0.0/0.0/15_003/0000477 financed from the ERDF. We also acknowledge CEITEC Nano Research Infrastructure supported by MEYS CR (LM2018110).

Reference

- [1] A. Danhel, F. Ligmajer, T. Sikola, A. Walcarius, M. Fojta, *J. Electroanal. Chem.* **2018**, 821, 53–59.
- [2] P. Havranova, F. Ligmajer, A. Danhel, *Electroanalysis* **2019**, 31, 1952–1960.
- [3] P. Sebest, L. Fojt, V. Ostatna, M. Fojta, A. Danhel, *Bioelectrochemistry* **2020**, 132, 107436.
- [4] P. Sebest, V. Ostatna, M. Fojta, A. Danhel, *J. Electroanal. Chem.* **2020**, Accepted 10.1.2020.
- [5] F. Ligmajer, M. Horak, T. Sikola, M. Fojta, A. Danhel, *J. Phys. Chem. C* **2019**, 123, 16957–16964.
- [6] A. Economou, *Sensors (Switzerland)* **2018**, 18, 1–23.
- [7] I. Jiranek, V. Cervený, J. Barek, P. Rychlovský, *Anal. Lett.* **2010**, 43, 1387–1399.
- [8] D. A. Malyshev, K. Dhami, T. Lavergne, T. Chen, N. Dai, J. M. Foster, I. R. Corrêa, F. E. Romesberg, *Nature* **2014**, 509, 385–388.

- [9] Y. Zhang, J. L. Ptacin, E. C. Fischer, H. R. Aerni, C. E. Caffaro, K. San Jose, A. W. Feldman, C. R. Turner, F. E. Romesberg, *Nature* **2017**, *551*, 644–647.
- [10] Y. Zhang, F. E. Romesberg, *Biochemistry* **2018**, *57*, 2177–2178.
- [11] J. Spacek, Y. Zhang, A. Danhel, F. Romesberg, M. Fojta, *Angew. Chemie Int. Ed.* **2020**, Under preparation.
- [12] A. W. Feldman, V. T. Dien, R. J. Karadeema, E. C. Fischer, Y. You, B. A. Anderson, R. Krishnamurthy, J. S. Chen, L. Li, F. E. Romesberg, *J. Am. Chem. Soc.* **2019**, *141*, 10644–10653.
- [13] T. Lavergne, M. Degardin, D. A. Malyshev, H. T. Quach, K. Dhimi, P. Ordoukhanian, F. E. Romesberg, *J. Am. Chem. Soc.* **2013**, *135*, 5408–5419.